ISSN 1330-3651 (Print), ISSN 1848-6339 (Online) https://doi.org/10.17559/TV-20210913080305
Original scientific paper

Analysis of Contact Surface Wear Performance of O-Ring Dynamic Seal Based on Archard Model

Yan ZHAO, Ziming FENG*, Yunchao LI, Li FENG, Qi LI, Wei CUI

Abstract: With the development of hydraulic system to high pressure gradually, the leakage risk of sealing system increases, and it is necessary to confirm the performance parameters of sealing structure through analysis and calculation. The traditional analysis of the friction and wear performance of the seal ring is limited to the amount of wear, and cannot describe the surface wear characteristics of the O-ring in detail. Based on the Archard model, this paper constructs a model to analyse and calculate the friction and wear performance of the dynamic seal structure through the material characteristics and operating parameters, analyses the friction and wear characteristics of the O-ring seal structure under different compression ratio, medium pressure, relative slip velocity and temperature, and summarizes the influence of each single variable on the wear characteristics of the dynamic seal structure. According to the analysis in this paper, the increase of medium pressure of 5 MPa will cause the wear concentration area of the contact surface to move to the back pressure side, and the overall wear will be reduced, but the increase of contact area will lead to the weakening of sealing effect. By the action of 15 MPa, when the compression ratio is between 5% and 10%, the change of cumulative wear rate and the wear rate of each node is small.

Keywords: archard model; dynamic seal; hydraulic seal; O-ring seal; wear

1 INTRODUCTION

Rubber O-ring is widely used in many fields. In order to give full play to the advantages of high energy density of hydraulic system, high pressure has become an important development direction. The most effective way to reduce the volume and weight of aircraft hydraulic system is to increase the working pressure. But high pressure brings leakage risk to the seal of hydraulic system. The life cycle and safety of the seal structure can be predicted by analyzing the change law of friction and wear of the seal.

The research of O-ring seal can be traced back to 1930, and many scholars use finite element numerical analysis and computational fluid dynamics to explore the friction law of reciprocating seal [1]. Zhang analyzed the influence of oil pressure, inner diameter tensile ratio, compression ratio and oil pressure difference between two sides of O-ring on the sealing performance of O-ring with the help of ANSYS, and concluded that von Mises stress is determined by oil pressure difference [2]. Xu analyzed the stress and failure forms of NBR O-ring in different working states through modeling, and concluded that the failure form in micro motion state depends on the moving speed [3]. Fujimoto studied the mechanical properties of the supporting structure composed of rubber O-rings, established an analysis method to predict the dynamic characteristics of O-rings without using any size related experimental data, and used Maxwell hyperelastic model to simulate the viscoelastic behavior of materials [5]. Peng and others used ABAQUS software to simulate based on the new 3-D model, and proposed an eccentric 3D fluid structure interaction model [6]. Salant calculated and compared the performance of various sealing forms based on Reynolds equation [7]. Nam proposed a hybrid method for photoelastic experiments by using the free boundary conditions of external forces and the relative equations of two stress functions in contact problems [8]. Schmidt established the theoretical model of mixed lubrication of O-ring sealing surface by ABAQUS software, but it was only limited to static load, not specific to dynamic load simulation [9]; Ong proposed using finite element method to solve the problems of axisymmetric fluid solid coupling and rubber stainless steel mixed lubrication in reciprocating seals [10]. At present, the simulation research of O-ring seal mainly focuses on the solution of stress and strain, while the analysis of dynamic seal wear performance is less.

In terms of wear simulation, Hasan proposed a prediction model of friction stir welding tool based on CFD [11], which is applicable to rigid body. Zhang used the method of setting the element separation to analyze the abrasive wear contact [12], but the unit wear of this method is limited by the minimum size of the element. Based on Archard model, Chang used ANSYS structural analysis and thermal analysis function to simulate the wear amount of O-ring [13], but did not analyze the specific wear characteristics of contact surface.

The above analysis model cannot describe the surface wear characteristics of O-ring in detail. Archard model is often used in cutting and welding simulation. It is a wear prediction model based on test. Based on the Archard model, this paper constructs a model to analyze and calculate the friction and wear performance of the dynamic seal structure through the material characteristics and operating parameters, analyzes the friction and wear characteristics of the O-ring seal structure under different compression ratio, medium pressure, relative slip velocity and temperature, and summarizes the influence of several variables on the wear characteristics of the dynamic seal structure.

The simulation model proposed in this paper can simulate the wear performance of the O-ring made of the material under the condition of known wear coefficient under specific working conditions. Based on O-ring dynamic seal structure, a two-dimensional model is built to analyze and calculate the friction and wear performance of dynamic seal structure by material characteristics and working conditions parameters. Different from the existing wear simulation methods, the accuracy of the results will not be interfered by the unit size, and the cumulative wear rate of contact surface can be displayed. The results show that the wear coefficient of the material is constant by default. If we want to get more accurate wear performance of O-ring by simulation, the wear coefficient of the related materials needs to be measured by experiments. The model can provide reference for the material selection and structural dimension determination of O-ring.

2 SIMULATION THEORY AND MODEL CONSTRUCTION

2.1 Analysis Process

In this paper, the contact analysis is carried out by using the finite element simulation method, and the wear analysis of the sealing structure is carried out by using the Archard model. The contact analysis process is as shown in Fig. 1.

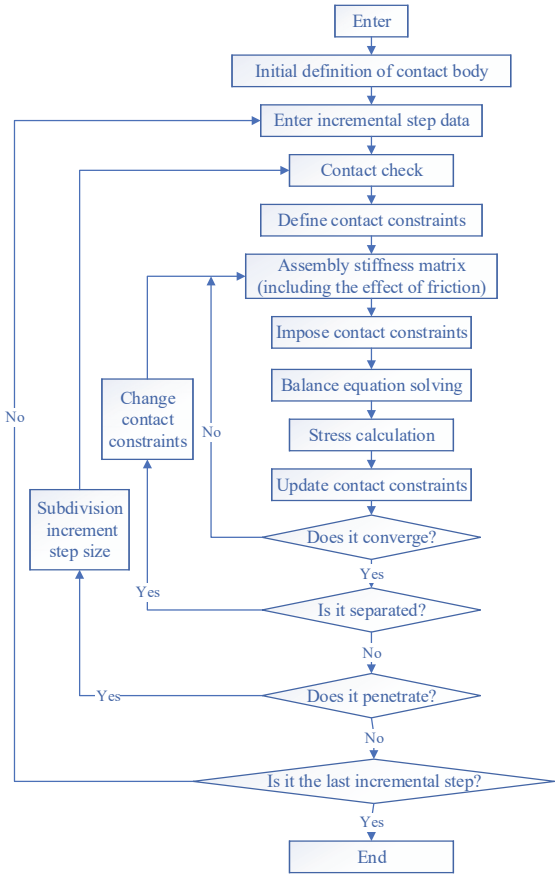

Figure 1 Finite element contact analysis process

2.2 Basic Theory

2.2.1 M-R Constitutive Model

Mooney theory is based on the following assumptions:

(1) Rubber is incompressible and isotropic before deformation.

(2) The simple shear process includes simple stretching, then simple shear superimposed on the plane section, and the whole process conforms to Hooke law.

On this basis, rivilin followed the above assumption and obtained the strain energy function through mathematical derivation:

$$W = C_1(\lambda_1^2 + \lambda_2^2 + \lambda_3^2 - 3) + C_2\left(\frac{1}{\lambda_1^2} + \frac{1}{\lambda_2^2} + \frac{1}{\lambda_3^2} - 3\right) \quad (1)$$

where:
W - strain energy;
λ_1, λ_2, λ_3 - strain rate of rubber along the three-dimensional direction;
C_1, C_2 - elastic parameters.

C_1 and C_2 can be obtained through experiments, and the material properties of rubber can be obtained by defining elastic parameters.

2.2.2 Archard Model

Archard model is a wear prediction model based on experiments [14].

The results show that the wear volume V, load W and sliding distance l have the following functional relationship [15]:

$$V = K_w WL \quad (2)$$

where:
K_W - wear coefficient of a specific material.

The wear resistance of friction materials can be measured by the wear coefficient. The wear coefficient can be understood as the volume wear caused by sliding unit distance under unit load. The wear coefficient K can be measured by test, and the calculation formula is as follows:

$$K = \frac{\Delta W}{d \cdot p \cdot V \cdot t} \ / \ \mathrm{cm}^3/\mathrm{Nm} \quad (3)$$

where:
ΔW - wear weight / g;
d - specific gravity of material / g/cm^3;
p - test load / N;
V - sliding linear velocity / m/s;
t - wear time / s.

Marc provides a wear analysis model, which can specify parameters related to wear analysis for deformable body. The wear model in Marc is based on Archard equation, which cannot be used for severe wear behavior. The model set up in this paper is applied to the hydraulic dynamic seal system, which usually fails when the amount of wear can be observed. It does not belong to severe wear, so the Archard model can be applied.

Archard model is as the following [11]:

$$w = KF\frac{G_t}{H} \quad (4)$$

where:
K - wear coefficient;
F - normal force;
G_t - slip distance;
H - hardness.

The above formula is transformed into incremental form, and the normal force is replaced by the normal stress (except the beam element). The simplified Archard equation can be obtained.

$$\dot{w} = \frac{K}{H} \cdot \sigma \cdot V_{\mathrm{rel}} \quad (5)$$

where:
$\dot{w}$ - wear change rate in the direction perpendicular to the surface;
σ - normal stress;
V_{rel} - relative sliding velocity.

2.2.3 Impact Factor Analysis

In the Archard model, the wear coefficient and hardness are the inherent characteristics of materials, and the normal stress and relative sliding speed are variables. In this simulation condition, the normal stress and compression ratio are related to the medium pressure. This paper will study the wear characteristics of rubber seal ring from three aspects: compression ratio, medium pressure and relative sliding speed. According to the actual working condition of aviation actuator, the gravity acceleration factor is introduced to analyze.

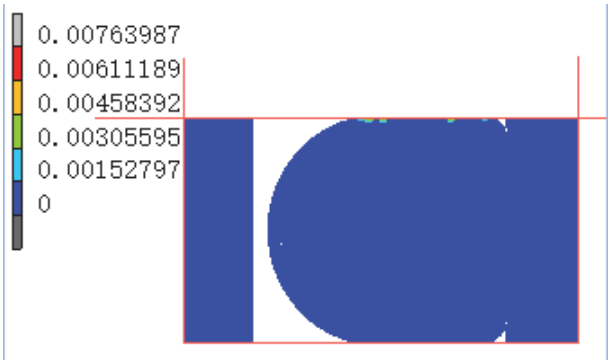

a) Cloud picture

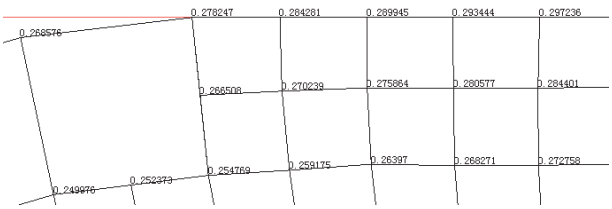

b) Node value

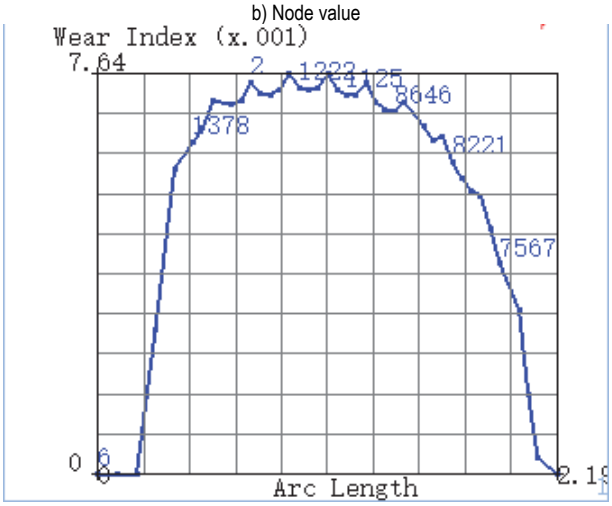

c) Numerical curve

Figure 2 Wear data set

In the process of numerical calculation, in an incremental step, the wear amount is, and the coordinate value of the node after wear should be adjusted accordingly, as shown in Fig. 2. Therefore, the analysis step should not be too large. In addition, if the wear accumulation is large, it needs to be remeshed. All solid element, shell element and beam element can be used in wear analysis. MARC and Mentat also have special variable output and display for wear results. It is mainly accumulated wear index and wear rate [16].

Wear rate refers to the loss of plastic samples after friction for a certain time or distance or a specified number of cycles.

The cumulative wear rate represents the wear ratio of the node in the direction perpendicular to the friction interface. This distance is in the O-ring wear structure model, that is, the distance between the outer wall and the inner wall of the groove. Therefore, the wear amount on the cross section can be obtained by fitting the wear rate curve, integrating and multiplying, as shown in the Eq. (6).

$$\Delta W = Wh\int_0^l w \tag{6}$$

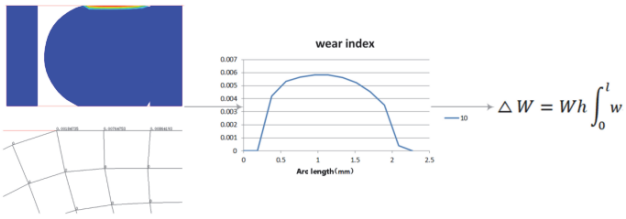

Figure 3 Calculation process of wear amount

As shown in Fig. 3, the unit wear amount can be obtained by dividing the total wear amount on the section by the total length of the unit. The total wear amount can be obtained by multiplying this value by the volume or mass of the original sealing ring. In the same way, the calculation method of total wear rate can be obtained.

2.3 Research Objects and Models

2.3.1 Research Objects

In this paper, the reciprocating seal structure of aviation hydraulic actuator is taken as the research object, and the working conditions and material parameters are set [17].

The operating parameters in Tab. 1 and implementation scheme are as follows:

Table 1 Basic parameters of sealing system [18]

O-ring	
Material	NBR
C10 / MPa	2.591-2.767
C01 / MPa	0.952-1.439
Cross section diameter *d* / mm	3.5
Stroke / m	0.3-0.75
Speed / m/s	0.1-0.25
Temperature / °C	25-120
Friction coefficient	0.05
Compression ratio / %	5-20
Retaining-ring	
Material	PTFE
Modulus of elasticity / MPa	280
Poisson's ratio	0.4
Width / mm	1
Piston rod and Cylinder wall	
Material	Rigid boundary
Working medium	
Pressure / MPa	5-20
Temperature / °C	25-120

Temperature: Because the temperature of the aviation hydraulic system changes greatly during operation, by consulting the relevant literature [18], it is known that the

O-ring is easier to wear under high temperature conditions. Therefore, this paper will focus on the wear of the sealing structure in the high temperature area. According to the rubber parameters set at 20 ℃, 80 ℃, 100 ℃ and 120 ℃, the material properties were analyzed.

Pressure: According to the national standard, the pressure of aviation hydraulic system is 5 ~ 28 MPa, and different hydraulic pressures will have an impact on the wear process of sealing structure. At present, the hydraulic system is mainly concentrated in the range of 10 ~ 25 MPa. Therefore, this paper sets the pressure interval as 5 MPa [19]. The maximum working pressure is 10 MPa, 15 MPa, 20 MPa and 25 MPa respectively. Simulate the hydraulic pressure supply mode under the actual working condition, and gradually increase the pressure from 0 to the maximum working pressure within 1 second.

Speed: set the speed by setting the position of the contact surface, and set it to uniform linear motion.

Realization mode: 1 control the pressing of contact surface in 1 second working condition to complete the loading action. Then, in 1 second to 2 seconds, the pressure is applied in the cavity in the opposite direction of the initial travel direction to complete the loading action. In 2 seconds to 5 seconds, the contact surface is set to move back and forth uniformly along the compression side.

2.3.2 Geometric Model

Because the O-ring seal structure is a revolving body, this paper can simplify the O-ring seal structure to a plane structure, as shown in Fig. 4.

The plane structure model of O-ring is imported into Marc for wear simulation. The model of size is shown in Fig. 4. The plane structure is used to construct the cross-section structure of O-ring to reserve space for loading deformation of O-ring and set the front and rear retaining rings. Ignoring the deformation of cylinder wall and groove, the two are set as rigid boundary.

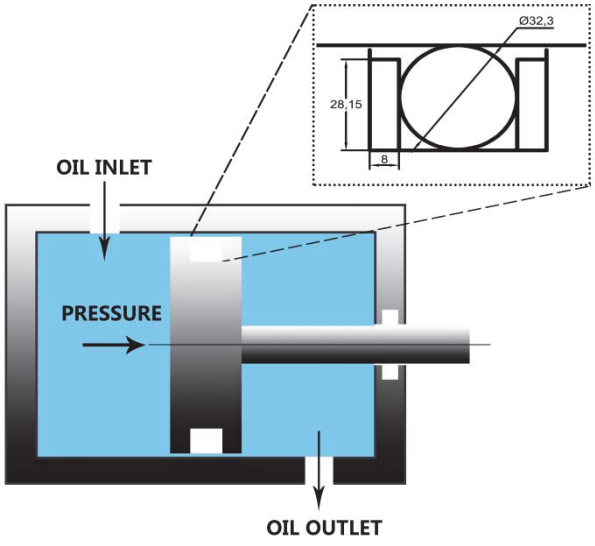

Figure 4 Plane structure of O-ring seal

The model setting process is shown in Fig. 5. The simplified model structure is constructed through the prototype of the sealing mechanism.

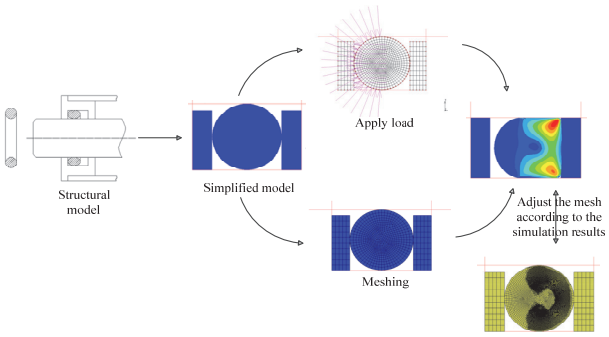

Figure 5 Simulation model setting process

The mesh is divided according to the simulation needs, and various boundary conditions including loads are imposed according to the working conditions and after the preliminary simulation, according to the problems in the post-processing.

2.3.3 Mesh Generation and Deformation Body Setting

Four node quadrilateral elements are selected for drawing, and the internal diffusion ratio is set to 0.9.

When meshing, the parts with large stress gradient are predicted to be meshed, and the other parts are meshed sparsely [20]. In order to avoid the abnormal results caused by the excessive stress and strain of individual elements in the calculation, the local remeshing is set. The position where the equivalent force or equivalent strain is greater than 50% is divided into two levels, and the position where 0.01 contact penetration occurs is divided into three levels. In the process of calculation, it is realized automatically with increment step. The function of contact analysis provided by Marc can ensure that the finite element mesh does not penetrate [21]. In results, the parameters including the remeshing are adjusted.

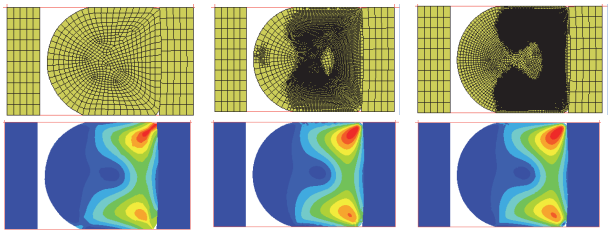

a) Number of grids 1859 No redivision | b) Number of grids 1859 Secondary redivision | c) Number of grids 6260 Secondary redivision

Figure 6 Cloud chart of mesh and maximum tensile stress under different mesh adaptive settings

As shown in Fig. 6, the models are set up to simulate under different grid density settings, and the maximum tensile stress result cloud diagram is derived. When the mesh number of the model is 1859 and the secondary mesh re division is carried out, the contour distribution in the cloud image is clear, and the error between the result and the result of the denser unit model is less than 0.2%, which can complete the wear simulation task.

The O-ring unit and the washer unit are respectively arranged. The O-ring unit is a deformable body, and the material is set as a rubber material based on Munirellin Coefficient; the washer unit is a deformation body, and the material is PTFE. Other locations are set as rigid boundaries.

Contact settings: the friction coefficient between O-ring and rigid boundary is 0.05, the friction coefficient between O-ring and retaining ring is 0.05, and the friction coefficient between retaining ring and rigid boundary is 0.05. The hardness of O-ring is 85 (unit), the wear coefficient is 0.0001, the wear scale factor with rigid boundary is 1, and the contact wear between O-ring and gasket is not considered. Set the friction type to Coulomb bilinear.

3 RESULTS AND DISCUSSION

3.1 Influence of Compression Ratio on O-Ring Seal Wear

Under the working conditions of 15 MPa, 25 ℃ and relative slip speed of 0.15m/s, the influence of compression ratio on the wear of O-ring seal is studied. The compression ratio is set as 5%, 10%, 15% and 20%, respectively, and the friction and wear analysis are carried out. The results are as follows:

It can be seen from Fig. 7 that when the compression ratio increases from 5% to 10%, the O-ring contacts the bottom of the groove, the working face contacts the back pressure side guard ring, and the pressure stress concentration occurs at the above-mentioned part.

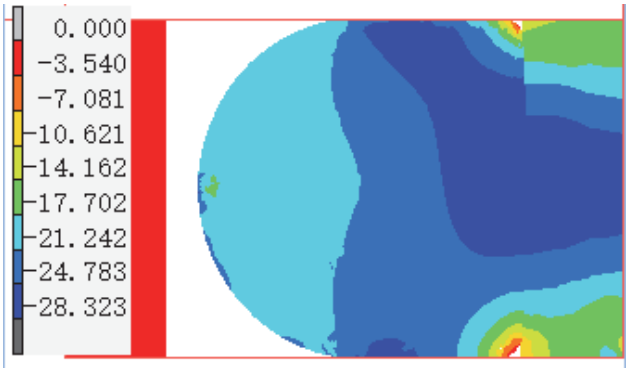

a) 5%

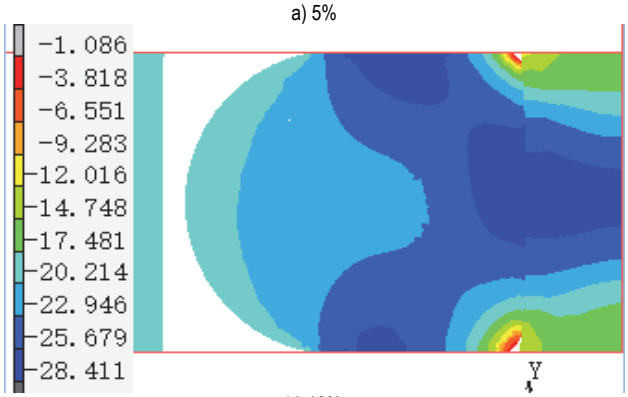

b) 10%

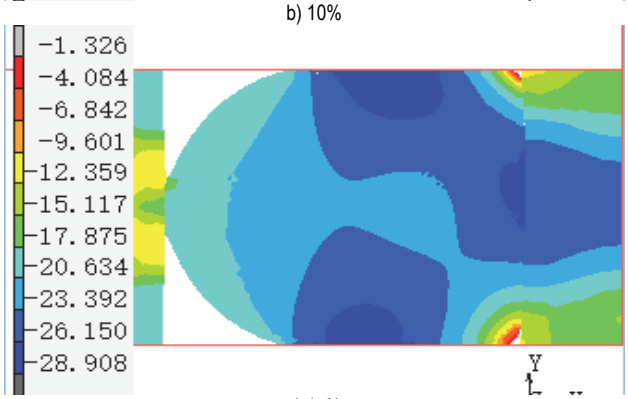

c) 15%

d) 20%

Figure 7 Cloud diagram of maximum main stress / MPa

When the compression ratio increases from 10% to 15%, the O-ring begins to contact the retaining ring on the pressure side, and a new stress concentration position appears after contact. This is because the internal stress of the O-ring increases significantly with the increase of the compression rate. Under the condition that other conditions remain unchanged, the O-ring is pressed by hydraulic pressure and attached to the surface of the retaining ring. The smaller the compression rate, the smaller the vertical deformation of the O-ring and the larger the horizontal deformation. When the compression rate is less than 15%, the O-ring stress is mainly affected by hydraulic pressure. When the compression rate is 20%, the horizontal deformation of the O-ring is too large, resulting in the extrusion of the retaining ring on both sides of the O-ring at the same time, resulting in a significant increase in its internal stress. By comparing Zhang's papers, it can be seen that the corresponding maximum von Mises stress under 1 MPa hydraulic pressure, 6%, 10% and 10% compression rate is 2.695 MPa, 2.841 MPa and 3.552 MPa. The maximum von Mises stresses corresponding to the compression rates of 5%, 10%, 15% and 20% under 28 MPa simulated in this paper are 28.323 MPa, 28.411 MPa, 28.980 MPa and 32.499 MPa respectively [22]. The variation law is basically the same, which shows that the simulation in this paper is effective.

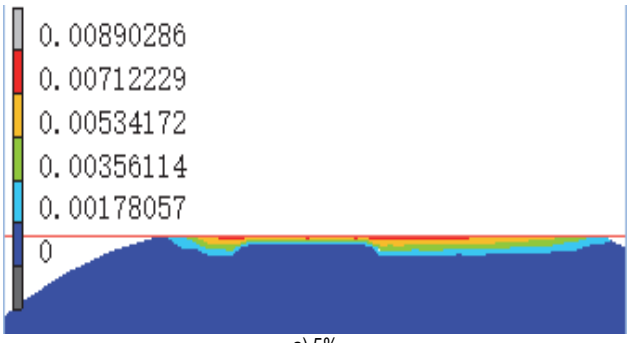

a) 5%

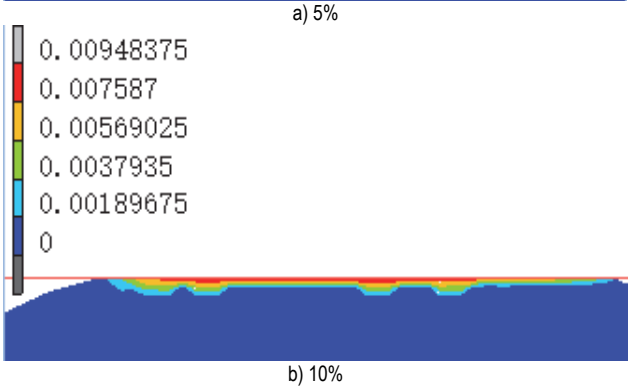

b) 10%

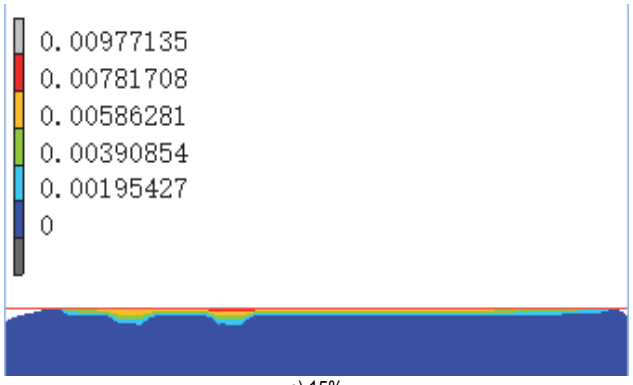

c) 15%

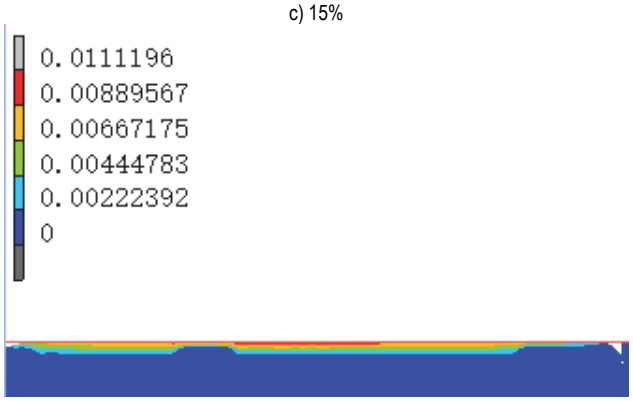

d) 20%

Figure 8 Cloud chart of cumulative wear rate

As shown in Fig. 8, with the increase of compression ratio, the contact area between O-ring and outer wall increases, and the wear position expands to both sides. The red part in the figure is seriously worn because the contact area between the cylinder wall and the O-ring gradually increases with the gradual increase of the compression rate, as shown in Fig. 8, resulting in the increase of the wear area of the O-ring. In addition, with the gradual increase of compression rate, the wear amount of O-ring increases accordingly. Under other conditions, the compression rate affects the contact pressure of O-ring. It can be seen from Eq. (5) that the stress affects the wear result of O-ring.

As shown in Fig. 9, when the compression ratio is between 5% and 10%, the value of cumulative wear rate has a positive proportional relationship with the compression ratio. With the increase of contact area, the main stress concentration position diffuses from the center to the reciprocating direction, and gradually increases from the back pressure side of the O-ring cylinder wall contact interface to the pressure side of the O-ring. The peak value of cumulative wear is located at the pressure side of the O-ring. Due to the limitation of groove space and the effect of medium pressure, the peak amplitude of cumulative wear rate decreases when the compression ratio increases from 10% to 15%.

When the compression ratio is small, the value of wear rate increases gradually from the back pressure side to the pressure side, and the peak value of wear rate moves to the pressure side. When the compression ratio increases to 15%, the peak value of wear rate begins to move to the pressure side. It can be seen from Fig. 9 that when the compression ratio increases from 10% to 15%, the global peak wear rate decreases. The peak value of wear rate continues to increase after the reverse transfer, and the speed is faster than that before the reverse transfer. The increase of wear rate with the increase of compression ratio is greater.

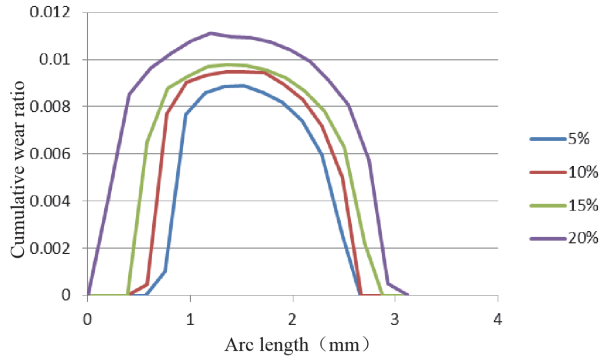

a) Cumulative wear rate

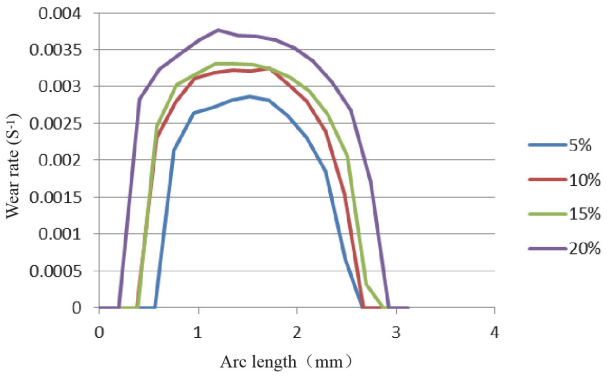

b) Wear rate

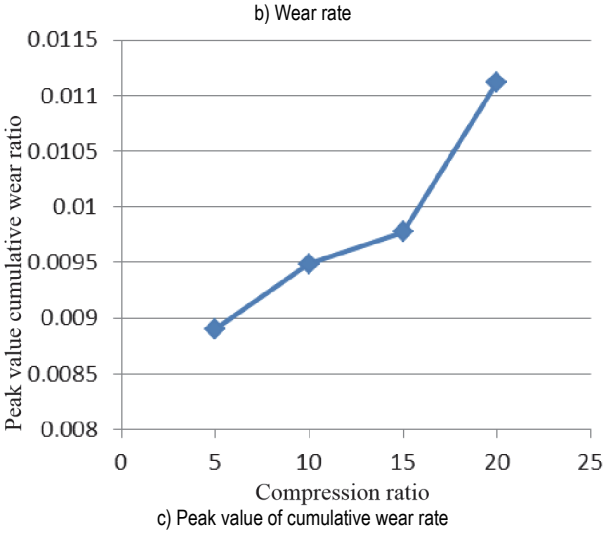

c) Peak value of cumulative wear rate

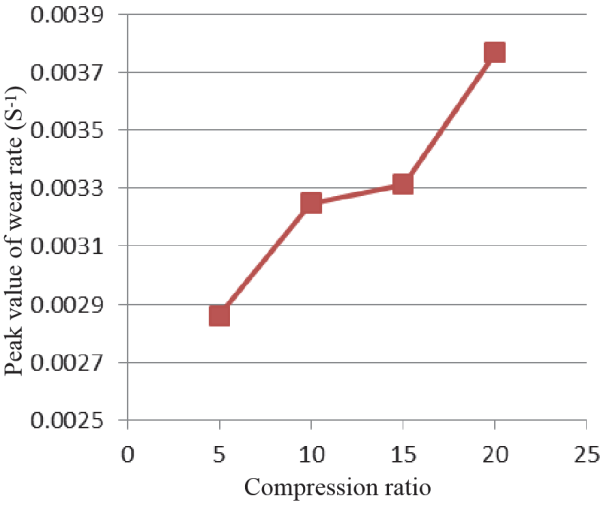

d) Peak value of wear rate

Figure 9 Cumulative wear rate and wear coefficient curve

The above results show that the compression ratio is positively correlated with the wear parameters. In the simulation experiment in this paper, when the compression ratio increases from 10% to 15%, the contact between the bearing side and the retaining ring occurs. It can be seen in Fig. 9c and Fig. 9d that this leads to the segmentation of the wear parameter curve, which indicates that the change trend of the wear parameters in the two states is different. It can be seen from Fig. 9c that the cumulative wear rate increases faster after the compression rate increases to 15%. In the maximum principal stress diagram, the O-ring structure changes from three-way compression to four-way compression, and the wear area remains unchanged during the transition from O-ring to four-way compression. In the three-way contact state, the wear position extends to the pressure side, while in the four-way contact state, the wear position extends to the pressure side and back pressure side.

3.2 Effect of Medium Pressure on O-Ring Seal Wear

By the working conditions of compression ratio 5%, temperature 25 °C and relative slip velocity 0.15 m/s, the effect of medium pressure on O-ring seal wear is studied. The medium pressure is set at 10 MPa, 15 MPa, 20 MPa and 25 MPa respectively, and the friction and wear analysis are carried out. The results are as follows:

It can be seen from Fig. 10 that the maximum principal stress increases linearly with the increase of pressure, and the increase is consistent with the medium pressure. At the same time, the O-ring is concentrated in the stress concentration area in the moving direction, and gradually diffuses in the opposite direction with the increase of medium pressure. This is consistent with Ye's research on the change law of O-ring under different hydraulic conditions [23]. Ye found that the internal stress of O-ring increases linearly with the linear increase of hydraulic pressure by increasing of hydraulic pressure, the same in this paper.

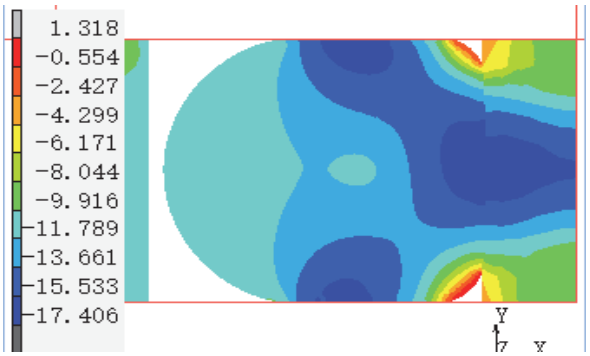

a) 10 MPa

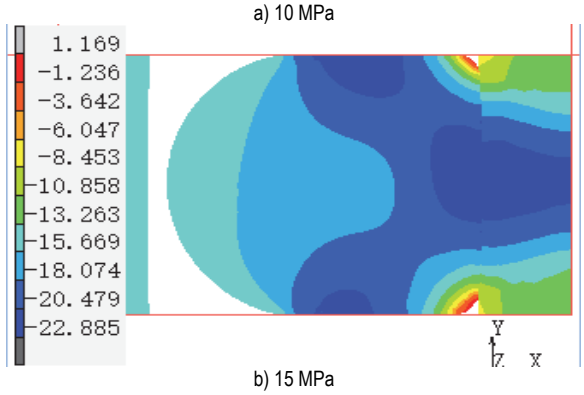

b) 15 MPa

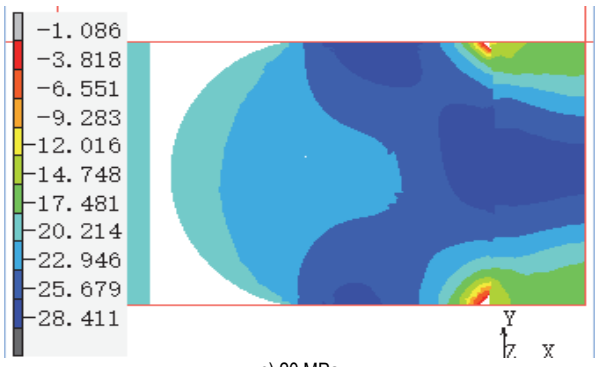

c) 20 MPa

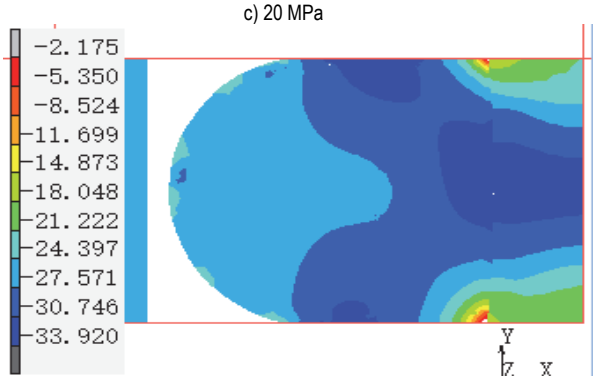

d) 25 MPa

Figure 10 Maximum principal stress nephograms

As shown in Fig. 11, the contact position remains unchanged, while the thinner part of the color band in the cloud image indicates that the stress and strain values at this position are more concentrated, and the lowest value is 50% of the global equivalent value. With the increase of medium pressure, the fold of contact surface is deepened, and the stress-strain concentration position is more dispersed than the high pressure state. The force on the O-shaped rubber ring increases, and the vertical internal stress of the O-shaped rubber ring increases with the hydraulic pressure increase. According to Eq. (5), the greater the stress, the greater the wear degree.

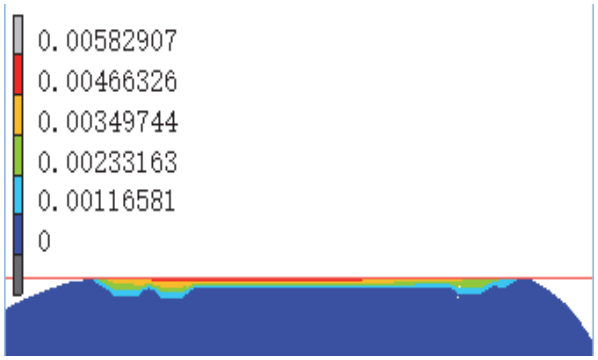

a) 10 MPa

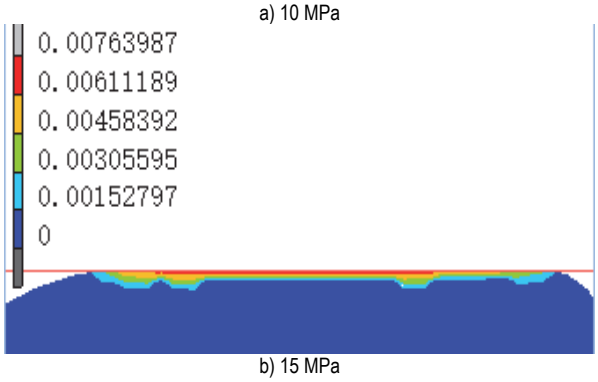

b) 15 MPa

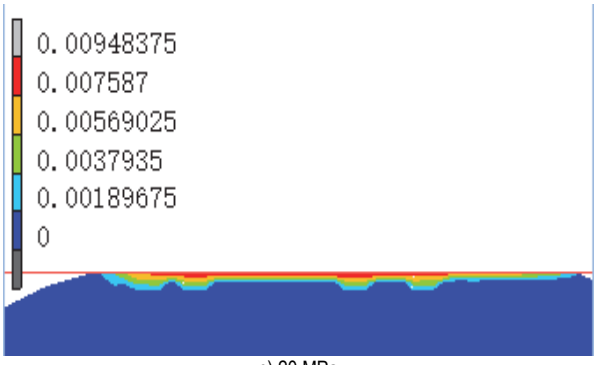

c) 20 MPa

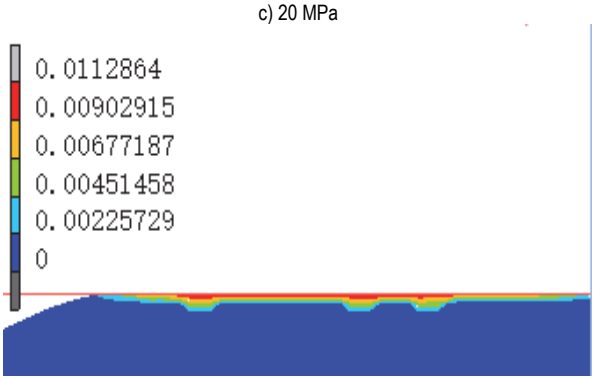

d) 25 MPa

Figure 11 Cloud diagram of cumulative wear rate

As shown in Fig. 12, the cumulative wear rate of O-ring is proportional to the change of medium pressure. When the pressure increases from 10 MPa to 15 MPa, the wear position expands to the back pressure side. When the pressure increases from 15 MPa to 20 MPa, the wear position extends to the pressure side. When the pressure increases from 20 MPa to 25 MPa, the wear position extends to both sides of pressure side and back pressure side.

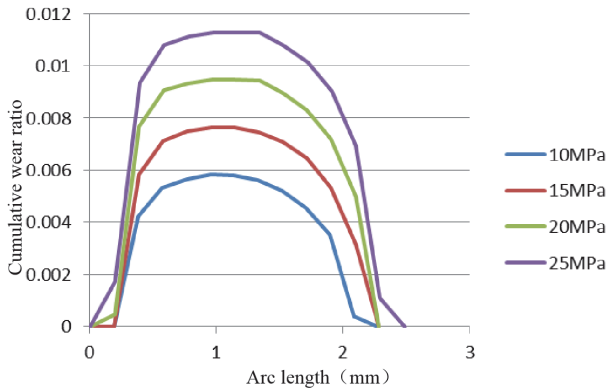

a) Cumulative wear rate

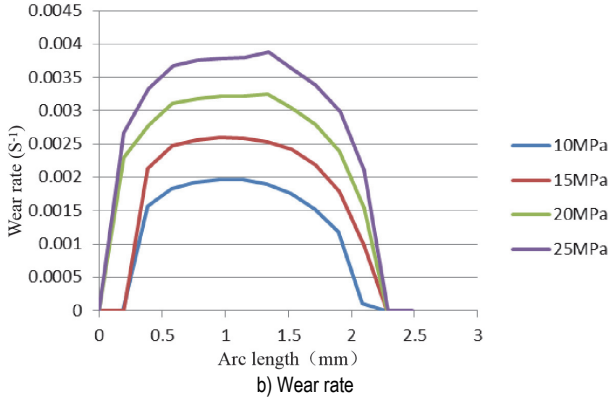

b) Wear rate

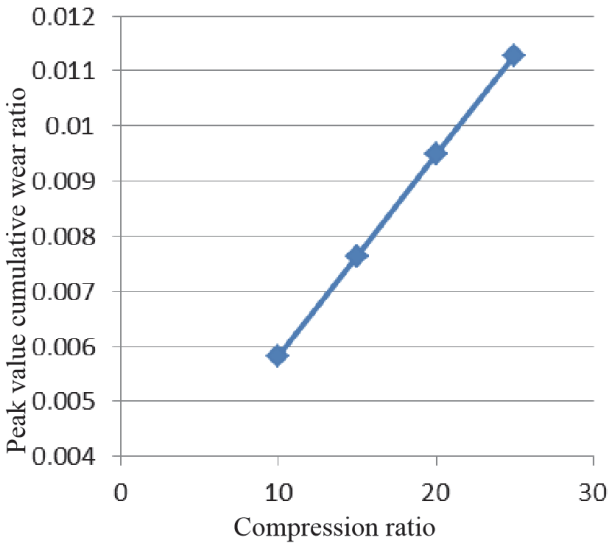

c) Peak value of cumulative wear rate

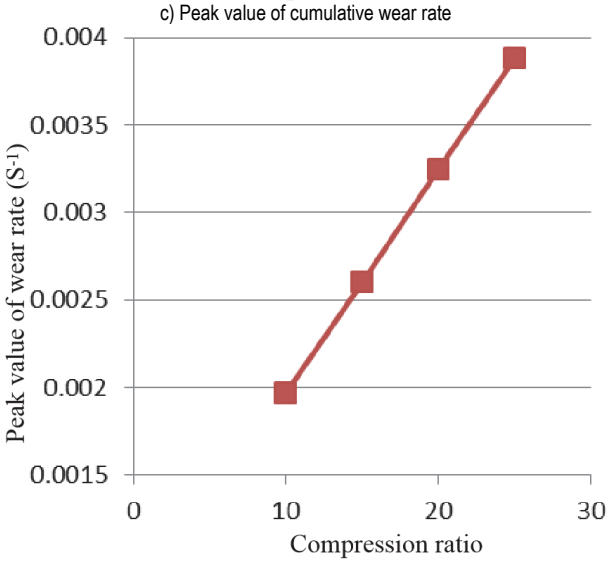

d) Peak value of wear rate

Figure 12 Cumulative wear rate and wear coefficient curve

When the load is 20 MPa, a small peak value of wear rate begins to appear on the back pressure side of O-ring, and the position of wear amount and peak value of wear rate on the contact surface of O-ring begins to move to the back pressure side. This means that under the high pressure environment, adjusting the working pressure can change the wear concentration position of the O-ring and prolong the service life of the sealing ring.

The results show that the change of stress has an obvious effect on the stress distribution of the seal ring. With the increase of the medium pressure, the maximum principal stress of the contact surface diffuses to both sides of the contact position, and the contact area increases. At the same time, the pressure of the contact surface increases. In terms of wear parameters, the medium pressure is positively proportional to the peak value of the cumulative wear rate and the peak value of the wear rate.

3.3 Effect of Relative Sliding Speed on O-Seal Wear

At the condition of compression ratio 5%, temperature 25 ℃ and medium pressure 15 MPa, the influence of relative sliding speed on the wear of O-ring seal was studied. Keeping the total reciprocating distance

unchanged, the reciprocating time was adjusted respectively, and the relative sliding speed was set as 0.1 m/s, 0.15 m/s, 0.2 m/s and 0.25 m/s, and the friction and wear analysis was carried out.

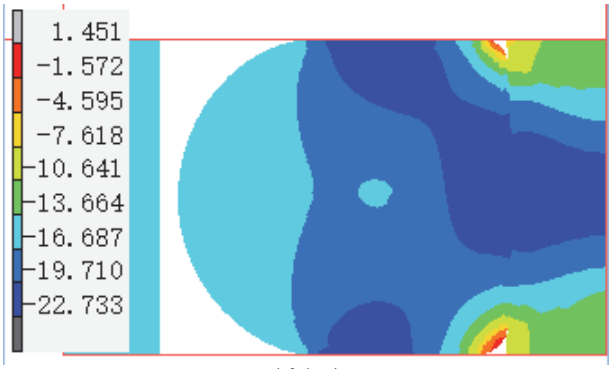

a) 0.1 m/s

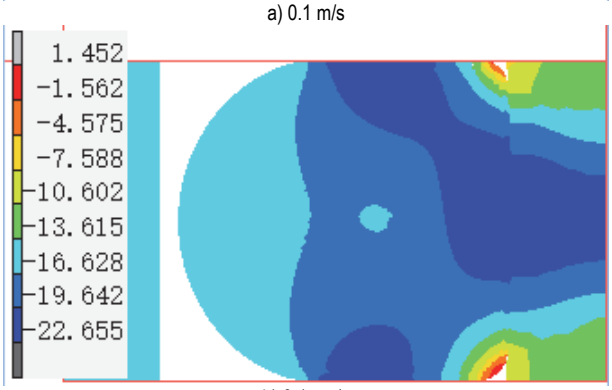

b) 0.15 m/s

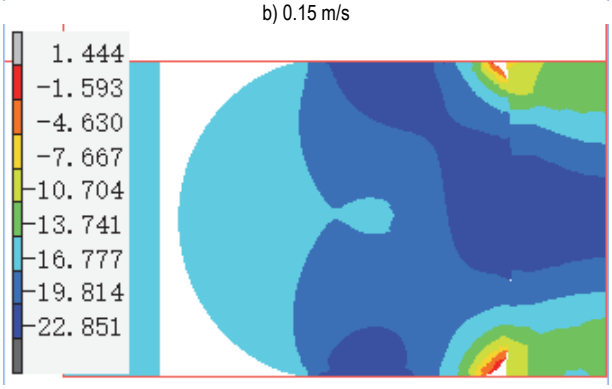

c) 0.2 m/s

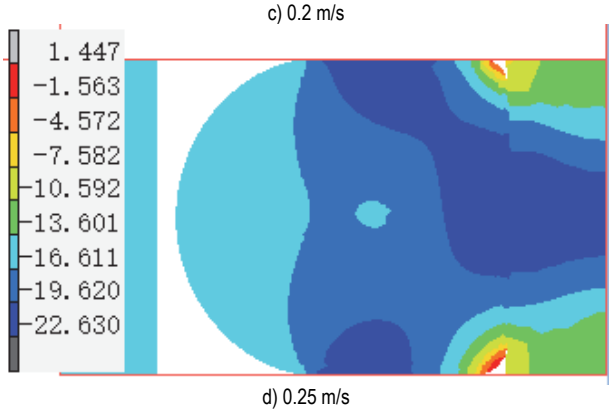

d) 0.25 m/s

Figure 13 Maximum principal stress nephograms

It can be seen from Fig. 13 that the change of speed has little effect on the internal stress of O-ring, the stress distribution has no obvious change, and the maximum pressure stress floating value is small. The simulation results show that the movement speed of piston has little effect on the stress of O-ring, which is consistent with the research results of Zhu [24].

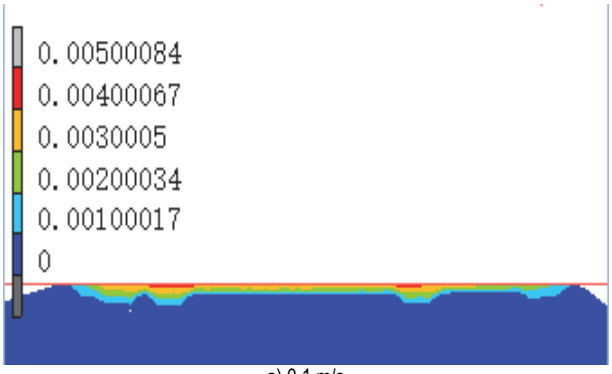

a) 0.1 m/s

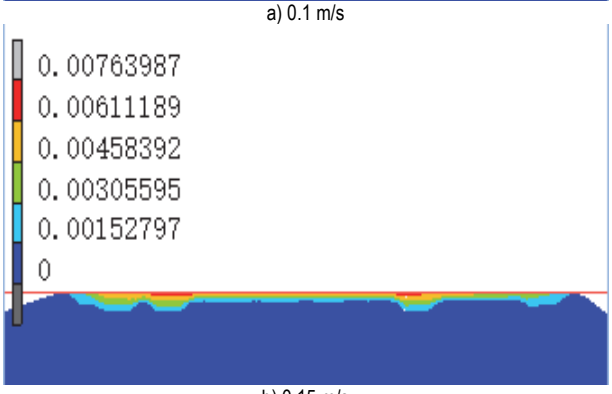

b) 0.15 m/s

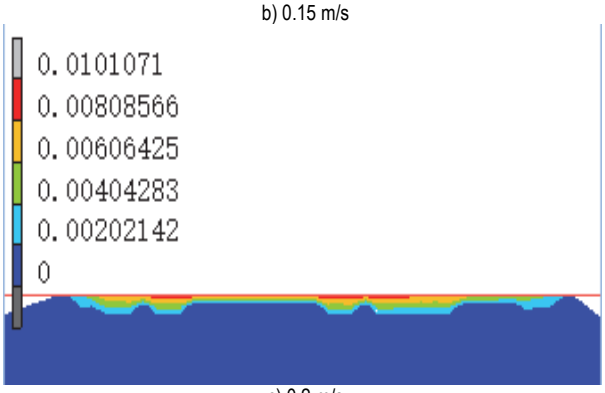

c) 0.2 m/s

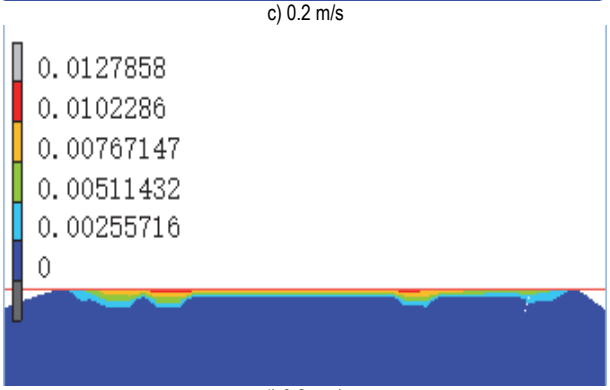

d) 0.25 m/s

Figure 14 Cloud diagram of cumulative wear rate

It can be seen from Fig. 14 that the wear position is evenly distributed on the contact surface, the distribution mode does not change significantly, and the stress-strain concentration position remains unchanged. Since the stress simulation results have little effect, it can be seen from Eq. (5) that the reciprocating speed of piston rod has little effect on the wear rate of O-ring.

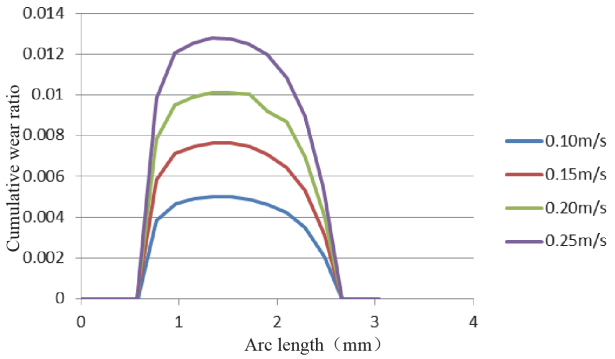

a) Cumulative wear rate

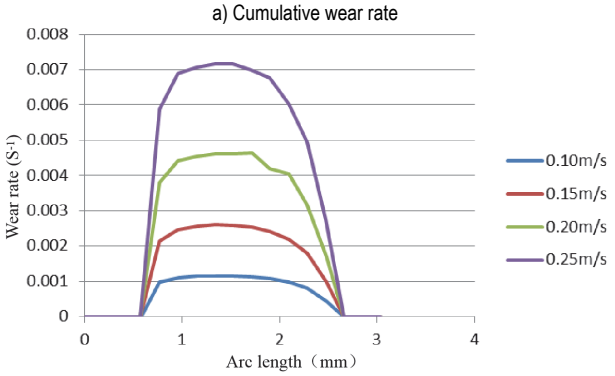

b) Wear rate

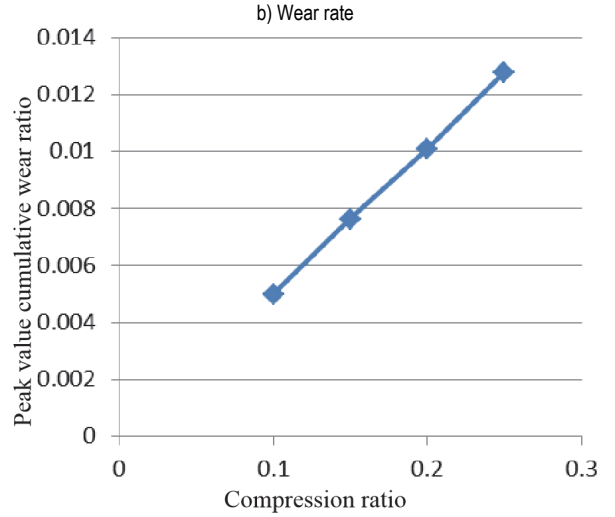

c) Peak value of cumulative wear rate

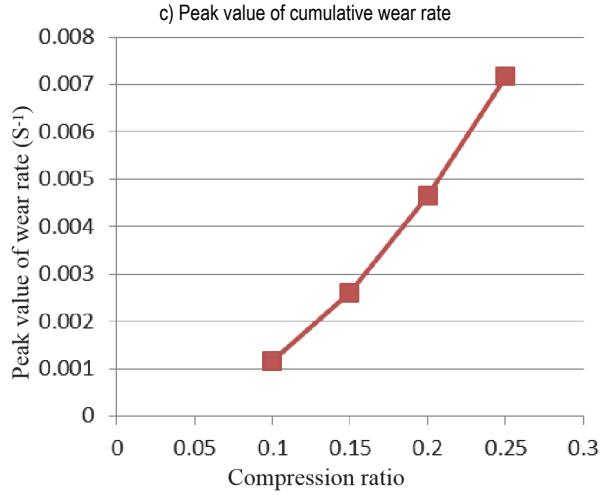

d) Peak value of wear rate

Figure 15 Cumulative wear rate and wear coefficient curve

It can be seen from Fig. 15 that when the speed changes, the internal stress of O-ring does not change obviously, but the peak value of cumulative wear rate changes obviously. Under the condition of the same displacement, the relative sliding speed is in direct proportion to the cumulative wear rate and relative wear rate. In the unit relative displacement, the faster the speed is, the more serious the wear of O-ring is. In the process of speed increasing, the node where the peak value of cumulative wear rate is located remains unchanged. The peak value of wear rate changes between two adjacent nodes and remains unchanged.

When the speed increases from 0.1 m/s to 0.25 m/s, the peak value of wear rate increases gradually, and the increase amplitude is slightly higher than the cumulative peak value of wear rate. It shows that the local wear of the dynamic seal structure is more serious when the speed increases.

The results show that the relative slip velocity is positively proportional to the cumulative wear rate and wear rate. With the increase of relative sliding speed, the cumulative wear rate of the corresponding position increases, and the slope of the growth curve is the wear coefficient of the corresponding sealing ring material.

3.4 Effect of Temperature on Wear of O-Ring Seal

The effect of temperature on the wear of O-ring seal was studied from the point of stress variation under the working conditions of 5% compression ratio, 0.15 m/s relative slip velocity and 15 MPa medium pressure. Tab. 2 shows munirelin parameters by different temperature conditions.

Table 2 M-R parameters of NBR [25]

Parameters	25 °C	80 °C	100 °C	120 °C
C10	2.767	2.658	2.643	2.591
C01	1.439	1.003	0.986	0.952

Set the material parameters of O-ring at 25 °C, 80 °C, 100 °C and 120 °C respectively, and analyse the friction and wear of O-ring. The results are as follows:

a) 25 °C

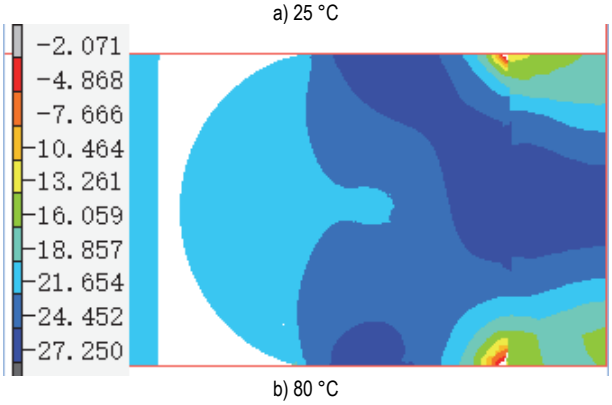

b) 80 °C

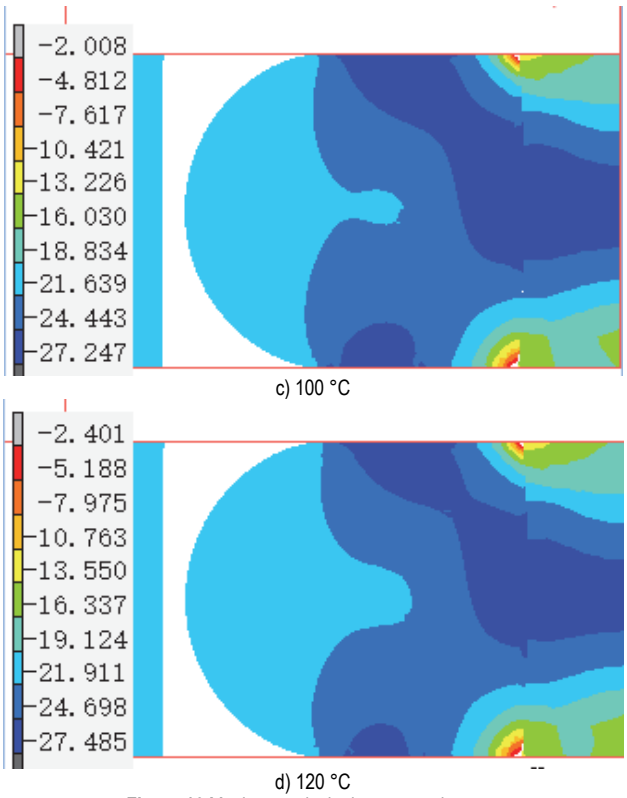

c) 100 °C

d) 120 °C

Figure 16 Maximum principal stress nephogram

It can be seen from Fig. 16 that the temperature rise has little effect on the principal stress distribution, and the maximum principal stress is mainly concentrated, which is still in the upper and lower contact positions. At 25 ℃, the maximum principal stress is higher than 80-120 ℃ in the high temperature region, but the maximum principal stress changes little in the high pressure region. It can also be seen from Zhang Bo's article that temperature basically has no effect on the stress of O-ring, and the only effect may be caused by the deformation of O-ring. When the O-ring increases from 0 ℃ to 80 ℃, the material gradually softens, the deformation increases significantly, some stress concentration areas are significantly relieved, and the stress is basically unchanged at 80-120 ℃ [26].

As shown in Fig. 17, the change trend of wear rate peak value with temperature change is divided into high temperature and low temperature ranges, which are 25 ℃ and 80-120 ℃ respectively. The wear value in high temperature range is obviously different from that in low temperature range, and the wear amount increases with the increase of temperature. However, the change of cumulative wear rate and wear rate is not obvious in the high temperature range. When the temperature increases from 80 ℃ to 100 ℃, the change of wear value is small. When the temperature increases from 100 ℃ to 120 ℃, the peak value of cumulative wear decreases and the peak value of wear rate increases. The wear rate changes little at 80 to 120 ℃, and the wear rate is mainly reflected in the effect of temperature on stress. The wear rate of O-ring can be calculated by Eq. (5).

As shown in Fig.18, the wear position does not change significantly with the change of temperature. The results show that with the increase of temperature, the rubber softens, the internal stress decreases, and the maximum principal stress decreases with the increase of temperature. The peak value of principal stress between 80 ℃ and 120 ℃ is significantly higher than that of 25 ℃.

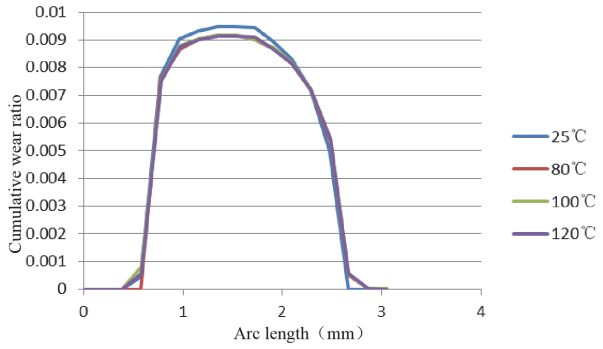

a) Cumulative wear rate

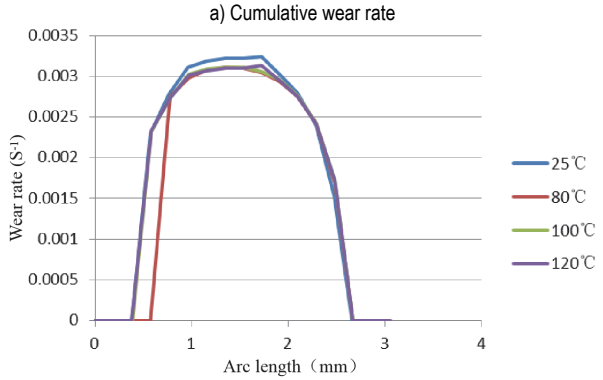

b) Wear rate

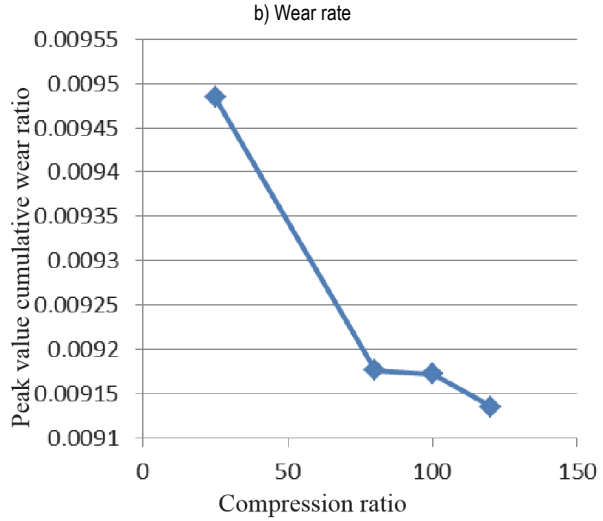

c) Peak value of cumulative wear rate

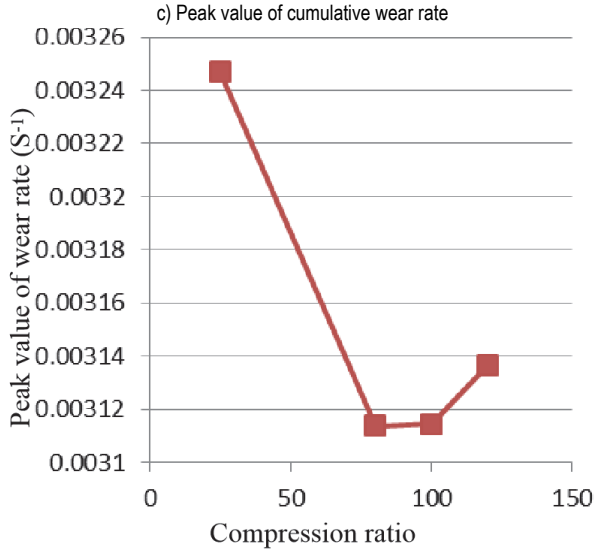

d) Peak value of wear rate

Figure 17 Cumulative wear rate and wear coefficient curve

Figure 18 Cloud chart of cumulative wear rate

It can be observed clearly from 25 ℃ to 120 ℃, but the curve of wear amount and wear rate peak value in 80 ℃ to 120 ℃ basically coincides, and the change is small. The cumulative wear rate peak value decreases, but the wear rate peak value rises. It can be seen from Fig. 18b to Fig. 18d that in 80 ℃ to 120 ℃, the material softening leads to the increase of contact area, and the wear position diffuses to the pressure side. The local wear increases, but the overall wear decreases.

The above results show that the increase of temperature will lead to the softening of O-ring material. Under the same conditions, the stress distribution position does not change, but the maximum principal stress decreases as a whole and the contact pressure decreases, resulting in the decrease of cumulative wear rate and wear rate. However, in the high temperature region, the continuous increase of temperature makes the O-ring soften further, and the overall cumulative wear rate increases, but the wear rate decreases during the heating process of the high temperature region, which indicates that the distribution of stress and wear on the contact surface is more uniform.

4 CONCLUSION

Based on the Archard model, the dynamic wear simulation model of O-ring seal structure of hydraulic actuator is established.

(1) For O-ring, the cumulative wear rate is positively correlated with wear rate, compression rate, medium pressure and relative sliding speed. While the wear coefficient remains unchanged, the temperature and cumulative wear rate are negatively correlated with wear rate;
(2) Under the action of 15MPa, when the compression ratio is between 5% and 10%, the change of cumulative wear rate and wear rate of each node is small;
(3) In the O-ring, the increase of contact area caused by the increase of compression ratio and medium pressure will reduce the efficiency of sealing effect;
(4) In the O-ring, the increase of the medium pressure will lead to the movement of the wear concentration area on the contact surface, which will reduce the overall wear and weaken the sealing effect;
(5) Adjusting the medium pressure in high pressure environment can change the wear concentration position of the sealing structure;
(6) When the speed increases, the local wear of dynamic seal structure is more serious.

Acknowledgment

The project was funded by the Natural Science Foundation of Heilongjiang province (No. LH2019E018; LH2021E020), Natural Science Foundation of China (No. 51774091), Heilongjiang Postdoctoral Scientific Research Developmental Fund (No. LBH-Q20083).

5 REFERENCES

[1] Ben, C. (2016). Rubber seal development via computer simulation. *Sealing Technology*, *1*, 8-12. https://doi.org/10.1016/S1350-4789(16)30017-4
[2] Liu, B. (2011). Finite element analysis of O-ring in servo actuator of a certain aircraft. *Lubrication Engineering*, *36*(06), 51-54. https://doi.org/10.1016/B978-0-444-53599-3.10005-8
[3] Xu, Q. (2018). Study on micromotion sealing and static sealing characteristics of NBR. *Refining and chemical industry*, *29*(06), 34-36. https://doi.org/10.16049/j.cnki.lyyhg.2018.06.013
[4] Szabo, G. & Varadii, K. (2018). Large Strain Viscoelastic Material Model for Deformation, Stress and Strain Analysis of O-rings. *Periodica Polytechnica Mechanical Engineering*, *62*(2), 148-157. https://doi.org/10.3311/PPme.11595

[5] Shoyama, T. & Fujimoto, K. (2018). Analytical Prediction of Dynamic Properties of O-Ring with Hydrostatic Pressure Distribution. *Journal of Applied Mechanics*, *85*(12), 121001. https://doi.org/10.1115/1.4041162
[6] Peng, C. (2018). Mixed Lubrication Modeling of Reciprocating Seals Based on a Developed Multiple-Grid Method. *Tribology Transactions*, *61*(6), 1151-1161. https://doi.org/10.1080/10402004.2018.1457750
[7] Salant, R. F., Yang, B., & Thatte, A. (2010). Simulation of hydraulic seals. *Proceedings of the Institution of Mechanical Engineers, Part J: Journal of Engineering Tribology*, *224*(9), 865-876. https://doi.org/10.1007/978-3-642-22647-2_100659
[8] Nam, J., Hawong, J., Han, S. et al. (2008). Contact stress of O-ring under uniform squeeze rate by photoelastic experimental hybrid method. *Journal of Mechanical Science and Technology*, *22*(12), 2337-2349. https://doi.org/10.1299/jsmeatem.2007.6._OS16-2-4-
[9] Schmidt, T., André, M., & Poll, G. (2009). A transient 2D-finite-element approach for the simulation of mixed lubrication effects of reciprocating hydraulic rod seals. *Tribology International*, *43*(10), 1775-1785. https://doi.org/10.1016/j.triboint.2009.11.012
[10] Öngün, Y. et al. (2008). An axisymmetric hydrodynamic interface element for finite-element computations of mixed lubrication in rubber seals. *Proceedings of the Institution of Mechanical Engineers, Part J: Journal of Engineering Tribology*, *222*(3), 471-481. https://doi.org/10.1243/13506501JET393
[11] Hasan, A., Bennett, C. J., Shipway, P. H. et al. (2017). A numerical methodology for predicting tool wear in Friction Stir Welding. *Journal of Materials Processing Technology*, 129-140. https://doi.org/10.1016/j.jmatprotec.2016.11.009
[12] Zhang, Y., Wang, J., Chen, F. et al. (2018). Contact thermal analysis of abrasive wear. *Lubrication Engineering*, *43*(10), 1-5. https://doi.org/CNKI:SUN:RHMF.0.2018-03-003
[13] Chang, K. (2018). Study on simulation method of O-ring wear based on ANSYS. *Chinese Hydraulics & Pneumatics*, *02*, 98-103. https://doi.org/CNKI:SUN:YYYQ.0.2018-02-023
[14] Archard, J. F. (1953). Contact and Rubbing of Flat Surfaces. *Journal of Applied Physics*, *24*(8), 981-988. https://doi.org/10.1063/1.1721448
[15] Kauzlarich, J. J. & Williams, J. A. (2001). Archard wear and component geometry. *Proceedings of the Institution of Mechanical Engineers, Part J: Journal of Engineering Tribology*, *215*(4), 387-403. https://doi.org/10.1243/1350650011543628
[16] Chen, H. H., Yu, J. Q., & Xi, Y. S. (2004). Msc. Marc/Mentat 2003 foundation and application examples. *Science Press*.
[17] TRELLEBORG. Airspace sealing system.
[18] Wang, H. M., Lv, X. R., & Wang, S. J. (2015). Effects of temperature on Swell and Wear Resistance properties of Nitrile Rubber in the Crude Oil. *Lubrication and sealing*, *40*(09), 30-34. https://doi.org/CNKI:SUN:RHMF.0.2015-09-007
[19] HB 6133-87. (1987). *Pulse test of hydraulic hose, conduit and connector assembly*. Beijing: Ministry of aviation industry of the people's Republic of China.
[20] Harvey, N. W., Martin, G. R., Mark, D. T. et al. (2000). Nonaxisymmetric Turbine End Wall Design: Part I-Three-Dimensional Linear Design System. *Journal of Turbomachinery*, *122*(2), 278-285. https://doi.org/10.1115/1.555445
[21] Zhao, X., Diao, X., Jiang, G. et al. (2019). Method for determining parameters of constitutive model of hydrogenated nitrile butadiene rubber. *China Synthetic Rubber Industry*, *42*(5), 352-356. https://doi.org/CNKI:SUN:HCXF.0.2019-05-007
[22] Zhang, B. S. (2001). Advanced Nonlinear Finite Element Analysis Software Marc for Contact Analysis. *Applied Science and Technology*, *12*, 36-39. https://doi.org/CNKI:SUN:YYKJ.0.2001-12-012
[23] Ye, W. L. (2019). *Quality control of sealability of underwater robot motor*. School of Mechanical Engineering Southeast University. https://doi.org/10.27014/d.cnki.gdnau.2019.004485
[24] Zhu, Q. H. (2017). *Theoretical and Experimental Study on Reciprocating Frictional Characteristics of Rubber O-ring*. Zhejiang University of Technology.
[25] Zhao, X. L. (2019). Method for determining parameters of constitutive model of hydrogenated nitrile butadiene rubber. *China Synthetic Rubber Industry*, *42*(05), 352-356. https://doi.org/CNKI:SUN:HCXF.0.2019-05-007
[26] Zhang, B. (2016). Analysis of the Influence of Temperature on the Stress of Rubber Sealing Ring. *Journal of Taiyuan University*, *34*(02), 14-16. https://doi.org/10.14152/j.cnki.2096-191X.2016.02.004

Contact information:

Yan ZHAO
School of Mechanical Science and Engineering, Northeast Petroleum University,
Daqing high-tech development zone university street No. 99, Daqing,
Heilongjiang Province, China
E-mail: 1475399070@qq.com

Ziming FENG
(Corresponding Author)
College of Mechanical and Electrical Engineering, Wenzhou University,
Chashan Higher Education Park, Ouhai District, Wenzhou City, 325000, China
E-mail: xueyuanfzm@163.com

Yunchao LI
National Pipeline Group Northern Pipeline Co., Ltd.,
No. 408, Xinkai Road, Guangyang District, Langfang, Hebei, China
E-mail: lych03@pipechina.com.cn

Li FENG
Research Institute of Oil Production Engineering,
Daqing Oilfield Co. LTD, China
E-mail: 672667782@qq.com

Qi LI
Research Institute of Oil Production Engineering,
Daqing Oilfield Co. LTD, China
E-mail: 741466073@qq.com

Wei CUI
Northeast Petroleum University,
Daqing high-tech development zone university street No. 99, Daqing,
Heilongjiang, China
E-mail: cuiweivv@126.com